



# Removal of Cationic Dye from Aqueous Solutions by Mauritanian Natural Kaolin Clay: Kinetic, Isotherm, Thermodynamic and Regeneration Studies

Aichettou Ibrahim Soko<sup>1</sup> · Abdoulaye Demba N'diaye<sup>1</sup> · M'hamed Taibi<sup>2</sup> · Marouane El Alouani<sup>2</sup> · Youssef Aoulad El Hadj Ali<sup>3</sup> · Jilali Aride<sup>2</sup> · Hamid Saufi<sup>2</sup> · Mohamed Kankou<sup>1</sup>

Received: 5 September 2022 / Accepted: 28 February 2023 / Published online: 3 April 2023  
© The Tunisian Chemical Society and Springer Nature Switzerland AG 2023

## Abstract

The objective of this work, was the valorization of Mauritanian natural kaolin clay. In this study, both structure and morphology were analyzed to determine the clay ability of adsorbance. The Effect of the operational parameters of the adsorption, using batch tests were studied. As a result, the Adsorption of MB appears to depend on the following factors: the mass of sorbent the pH of solution, contact time, initial dye concentration and temperature. The pseudo-second order model described the kinetic data quite well. The Langmuir model was found adequate to provide a better description of the isothermal data, and to determine the monolayer maximum adsorption ability. Furthermore, the MB adsorption into kaolin was spontaneous and exothermic as found by the thermodynamic parameters. Moreover, the reusability test showed the stability, and reusability of the natural clay after 4 cycle of adsorption process. The results of all performed analyses, affirm that the kaolin clay adsorbent could be effectively used as an alternative and low-cost material for cationic dye removal from industrial wastewater.

**Keywords** Kaolin clay · Methylene blue dye · Characterization · Adsorption · Reusability

## 1 Introduction

The pollution of the surface and groundwater sources is becoming more of a widespread problem that affects worldwide countries. The volume of fresh water supplied to the entire industry, agriculture and households have dropped drastically over the years. This is due to assorted reasons including, the number of dangerous wastes which has been increased as to synthesized dyes in water resources, the discharge of dye effluents from industries such as textile, paper industry, cosmetic, food, technology, so on without any

treatment, all of which play a key part into water resources contaminations [1].

However, several techniques have been used to remove hazardous dye from water due to its harmful effects, including, photodegradation [2], coagulation-flocculation [3], reverse osmosis [4], electrochemical oxidation [5], ozonation [6], solvent extraction [7]. The high expense and manufacturing complication of these materials limits their large-scale use [8].

Over the past few decades, the adsorption process with activated carbon has remained one of the most efficient and compelling proposals for the removal of dye-contaminated wastewater [9, 10]. This is considered an economical alternative since it does not necessitate any extra pre-treatment steps if inexpensive adsorbents are used [11]. In this aspect, a lot of recent research has focused on finding an economical and accessible bio adsorbent alternative to replace activated carbon, as it is expensive and difficult to regenerate [12].

Recently, the use of clays as alternative adsorbents has drawn attention to dye removal from wastewater [13–16]. Their low cost, as well as their adsorption properties, present an advantage compared to other commercially available adsorbents. The use of locally available sewage sludge has

✉ Abdoulaye Demba N'diaye  
abdouldemba@yahoo.fr

<sup>1</sup> Unité de Recherche, Eaux Pollution et Environnement, Faculté des Sciences et Techniques, Université de Nouakchott Al-Aasriya, BP 880, Nouakchott, Mauritania

<sup>2</sup> Université Mohammed V de Rabat, Centre des Sciences des Matériaux (CSM), (LPCMIO), Ecole Normale Supérieure, BP 10200, Rabat, Morocco

<sup>3</sup> Department of Chemistry, Faculty of Science, University Abdelmalek Essadi, B.P. 2121, Mhannech II, 93002, Tetouan, Morocco

considerable economic and environmental advantages. Consequently, several inexpensive adsorbents used to remove Methylene Blue (MB) from wastewater are reported in the literature [17, 18].

MB is a basic dye extensively used for cotton and silk painting. The most common harmful effect of MB is eye burn since it is thought to be the cause of permanent injury to eyes. It is also evident to cause mental confusion, profuse sweating, vomiting, nausea, breathing problem, and methemoglobinemia [19].

Therefore, the main objective of this research work, is to determine the feasibility of employing a local Mauritanian clay to remove MB from aqueous solutions. The influence of various operational parameters on the adsorption of MB dye onto kaolin clay, such as the adsorbent mass, pH of the solution, contact time, initial MB concentration was conducted. The clay physicochemical properties before and after adsorption of MB were also probed to understand the adsorption behavior of MB on Mauritanian kaolin clay. Several kinetics models of adsorption including pseudo-first order, and pseudo-second order models are implemented. The isothermal constants for the Langmuir, Freundlich and Temkin models were obtained by linear regression analysis. Thermodynamic parameters, such as  $\Delta G^\circ$ ,  $\Delta H^\circ$  and  $\Delta S^\circ$  were also calculated. The reusability of the clay after several MB dye adsorption cycles was further evaluated and discussed. Further the adsorption abilities of natural Mauritanian kaolin clay as a low-cost adsorbent were then compared with the ones reported in the literature.

## 2 Material and Methods

### 2.1 Adsorbent and Adsorbate

Natural kaolin clay was collected from the Hassi El Ebyed in Moughataa of M'Bout, Wilaya of Gorgol region (Mauritanian). The raw natural clay was sieved and the fraction below 200  $\mu\text{m}$  was collected, and dried at 105  $^\circ\text{C}$  in an oven. This raw material was used for all adsorption tests without any further modification and treatment. MB dye was obtained from Sigma–Aldrich, Germany (MW: 319.86 g/mol, purity  $\geq 99.00\%$ ).

### 2.2 Characterization and Analysis of Natural Clay

The pH, moisture, Swelling index, and loss mass ignition are determined by described methods [20]. The bulk density was determined using a picnometer [21]. X-Ray Fluorescence (XRF) using spectrometer-Type Axios was applied for the identification of the chemical composition of natural clay. Meanwhile The mineralogical composition of natural clay was determined by X-ray diffraction with Xpert Pro model

diffractometer equipped with a source operating Cu-K $\alpha$  (1.54060 Å). Fourier Transform Infrared (FTIR) spectroscopy (Bruker Platinum ATR) in the range of 4000–400  $\text{cm}^{-1}$  wavelengths was also used to identify the samples functional groups. There was also a use of the Scanning electron microscopy (SEM) coupled with energy-dispersive X-ray spectroscopy (EDX) analysis (JEOL-6300F) to visualize the microstructure and morphological characteristics of natural clay. Differential Scanning Calorimetry (DSC) was carried out in a temperature ranged from 100 to 750  $^\circ\text{C}$  with a heating rate of 10  $^\circ\text{C min}^{-1}$  under argon atmosphere by using a SETARAM 121 apparatus. The pH at the point of zero charge ( $\text{pH}_{\text{pzc}}$ ) of the natural clay was determined by the method described by El Alouani et al. [22]. A series of (0.01 M)  $\text{KNO}_3$  solution ( $V = 100 \text{ mL}$ ) were prepared, and the initial pH of  $\text{KNO}_3$  was adjusted to a given value from pH 2 to 13 by the addition of HCl (0.1 M) or NaOH (0.1 M). To each solution, 0.1 g of geopolymer was added and shaken for 48 h with an agitation speed of 120 rpm at room temperature. The differences between the pH value of the initial solution ( $\text{pH}_i$ ) and the final solution ( $\text{pH}_f$ ) were plotted as a function of  $\text{pH}_i$ . The point of intersection of this curve yielded the point of zero charge.

### 2.3 Batch Adsorption Experiments

Different sort of adsorption experiments was performed of MB dye onto natural clay in a batch system, and that include the adsorbent mass (0.025–0.175 g), solution pH (2.7–12), contact time (0–180 min), initial MB dye concentrations (20–80  $\text{mg L}^{-1}$ ), and temperature (20–50  $^\circ\text{C}$ ). The evaluation of adsorption process was done in a thermostatic batch by adding 0.1 g of clay to 50 mL of MB dye with initial concentration of 20  $\text{mg L}^{-1}$ . The pH solution was adjusted using HCl (0.1 M) or NaOH (0.1 M) and measured by the pH-meter Milwaukee model (Mi 150). After equilibrium, the mixture (adsorbate-adsorbent) was separated using centrifugation (Centrifuge ROTOFIX 32A) at 4000 rpm for 10 min. The spectrophotometer (JASCO V-630 UV–Vis–NIR model) at  $\lambda_{\text{max}} = 663 \text{ nm}$  was apply to determine the MB residual supernatant concentration.

The MB dye percentage removal from aqueous solutions is determined by Eq. (1), while the adsorbed amount at any time  $q_t$  ( $\text{mg g}^{-1}$ ), and  $q_e$  ( $\text{mg g}^{-1}$ ) at equilibrium were calculated using Eqs. (2) and (3), respectively:

$$\text{Removal (\%)} = \frac{C_i - C_e}{C_i} \times 100 \quad (1)$$

$$q_t = \frac{(C_i - C_t)V}{m} \quad (2)$$

$$q_e = \frac{(C_i - C_e)V}{m} \quad (3)$$

where  $C_0$ ,  $C_t$ , and  $C_e$  ( $\text{mg L}^{-1}$ ) represent the concentrations of MB dye at the initial time, at the time  $t$ , and the equilibrium time, respectively. the  $V$  (L) is the volume of MB dye solution, and the  $m$  (g) is the adsorbent mass.

## 2.4 Adsorption Kinetics

Several kinetic adsorption models were used to examine the mechanism and adsorption rate in the adsorption study. In this work the rate of adsorption in the solid phase (adsorbate) was obtained using the pseudo-first-order (PFO) which is usually applicable in the first minutes of the adsorption process. this model can be a monitoring step to the mechanism of adsorption [23] the linear form of this model was represented by Eq. (4):

$$\log(q_e - q_t) = \log q_e - \frac{k_1}{2.303}t \quad (4)$$

The pseudo-second order kinetic model (PSO) predicted that the hypothesis of the rate-limiting step can be chemisorption, implying either an exchange or a valence force, through electron sharing between the adsorbate (inorganic or organic pollutants) and the adsorbent (solid surface). The linear form of this model was given by the following Eq. (5):

$$\frac{t}{q_t} = \frac{1}{k_2 q_e^2} + \frac{t}{q_e} \quad (5)$$

where  $q_e$  and  $q_t$  are the quantities of MB adsorbed ( $\text{mg g}^{-1}$ ) on the adsorbent at equilibrium and time  $t$ , respectively.  $k_1$  ( $\text{min}^{-1}$ ),  $k_2$  ( $\text{g mg}^{-1} \text{min}^{-1}$ ) are a PFO and PSO constants respectively.

## 2.5 Adsorption Isotherms

The evaluation of the nature and homogeneity of the adsorbate layer on the surface of the adsorbent was performed with the investigation of different isotherm adsorption models. The Langmuir, Freundlich, as well as Temkin models were the ones often used for isothermal modelling in adsorption process [23]. The Langmuir model (where all adsorption sites assumed to be homogeneous, energetically equivalent and identical) was used to investigate the maximum adsorption capacity which correlate the saturation of the clay surface and can be calculated using the linear form of Langmuir isotherms. The Eq. 6 represents the linier mode of langmuir model.

$$\frac{C_e}{q_e} = \frac{C_e}{q_e} + \frac{1}{K_L q_m} \quad (6)$$

where  $C_e$  ( $\text{mg/L}$ ) is the equilibrium concentration of MB dye in solution,  $q_e$  ( $\text{mg g}^{-1}$ ) is the equilibrium uptake of MB dye on the adsorbent surface,  $q_{\text{max}}$  ( $\text{mg g}^{-1}$ ) is the maximum monolayer retention of MB dye on the adsorbent surface and  $K_L$  ( $\text{L mg}^{-1}$ ) is the Langmuir constant that refers to the energy of adsorption process. The separation factor  $R_L$  was used for the characterization of the Langmuir isotherm model, which was calculated by the following Eq. (7):

$$R_L = \frac{1}{1 + K_L C_0} \quad (7)$$

The adsorption process is unfavorable when ( $R_L > 1$ ), favorable when ( $0 < R_L < 1$ ), linear when ( $R_L = 1$ ) and irreversible when ( $R_L = 0$ ).

Freundlich isotherm model (adsorption sites varying in interaction with adsorbate) is appropriate for those mechanisms where multilayer adsorption occurs due to heterogeneous system. The Linear form of Freundlich isotherm model can be symbolized as:

$$\text{Ln}q_e = \text{Ln}K_F + \frac{1}{n} \text{Ln}C_e \quad (8)$$

where  $C_e$  ( $\text{mg L}^{-1}$ ) is the equilibrium concentration of MB dye,  $q_e$  ( $\text{mg g}^{-1}$ ) is the amount adsorbed on the adsorbent at equilibrium,  $K_F$  ( $(\text{mg g}^{-1}) (\text{L mg}^{-1})^{1/n}$ ) is the Freundlich adsorption constant and  $n$  is the heterogeneity factor showing the capacity of adsorption onto adsorbent and the adsorption strength between adsorbent-adsorbate. The parameter value of  $n$  reveals the favorability of the adsorption process, the reaction is favorable if the values of  $n > 1$  and it is unfavorable if  $n < 1$ .

We further investigated Temkin model for the adsorption of dye onto clay to examine the interaction between adsorbate adsorbent. This model is expressed by the following Eq. 9:

$$q_e = B \text{Ln}K_T + B \text{Ln}C_e \quad (9)$$

where  $B$  ( $\text{J mol}^{-1}$ ) is a constant related to the adsorption energy and  $K_T$  ( $\text{L mg}^{-1}$ ) is the Temkin isotherm constant.

## 2.6 Thermodynamic Study

In the thermodynamic study, standard change Gibbs free energy ( $\Delta G^\circ$ ) ( $\text{J mole}^{-1}$ ), enthalpy ( $\Delta H^\circ$ ) ( $\text{J mole}^{-1}$ ) and entropy ( $\Delta S^\circ$ ) ( $\text{J.K}^{-1} \text{mol}^{-1}$ ) parameters used for the determination of the nature, feasibility, favorability of the adsorption process. The values of  $\Delta G^\circ$ ,  $\Delta H^\circ$ , and  $\Delta S^\circ$  were calculated as following:

$$K_d = \frac{q_{ads}}{C_e} \quad (10)$$

$$\ln(K_d) = -\frac{\Delta H^0}{RT} + \frac{\Delta S^0}{R} \quad (11)$$

$$\Delta G^0 = \Delta H^0 - T\Delta S^0 \quad (12)$$

$C_e$  ( $\text{mg L}^{-1}$ ) is the concentration of dye at equilibrium,  $q_{\text{ads}}$  ( $\text{mg g}^{-1}$ ) is the amount of dye adsorbed on the adsorbent at equilibrium,  $K_d$  ( $\text{L mg}^{-1}$ ) is the thermodynamic distribution coefficient,  $T$  (K) is the absolute temperature and  $R$  ( $8.314 \text{ J mol}^{-1} \text{ K}^{-1}$ ) is the universal gas constant.

## 2.7 Regeneration and Reusability of the Adsorbent

The regeneration of adsorbents is important from an economical point of view; the adsorbents recycling is considered as an important aspect to minimize the costs related to the synthesis of materials. The natural clay sample after adsorption of MB dye was heated up to  $400^\circ\text{C}$  for 2 h (for MB dye decomposition), the sample was reused and the percentage removal was determined using  $20 \text{ mg L}^{-1}$  MB solution. Many cycles of regeneration were performed, followed by FTIR and DSC analyses to evaluate the stability of the adsorbent after regenerations.

## 3 Results and Discussion

### 3.1 Characterization of Natural Clay

#### 3.1.1 The Physico-Chemical Properties of Kaolin Clay

The physical and chemical properties of kaolin clay are listed as following: pH 7.95, moisture 1.49%, Bulk density 0.83, Swelling index 1.03 and Loss on ignition 30.11%.

#### 3.1.2 X-ray Fluorescence Analysis

The chemical composition of clay kaolin, determined by X-ray fluorescence method, (by mass %) is  $\text{SiO}_2$  42.098%,  $\text{CaO}$  0.081%,  $\text{Al}_2\text{O}_3$  18.573%,  $\text{Fe}_2\text{O}_3$  5.96%,  $\text{MgO}$  0.151%,  $\text{K}_2\text{O}$  0.176%,  $\text{Na}_2\text{O}$  0.05%,  $\text{P}_2\text{O}_5$  0.115%,  $\text{SO}_3$  0.22%,  $\text{MnO}$  0.013% and  $\text{TiO}_2$  1.2999%. These results showed that the predominant constituents are Silica and Aluminium oxide and other elements in minor quantities such as iron, titanium, sulfate, potassium, magnesium, phosphor, calcium, sodium, and manganese oxides considered as impurities.

#### 3.1.3 XRD Analysis

For the identification of the crystalline phases in the prepared material, XRD analysis was performed, the results of which are shown in Fig. 1.

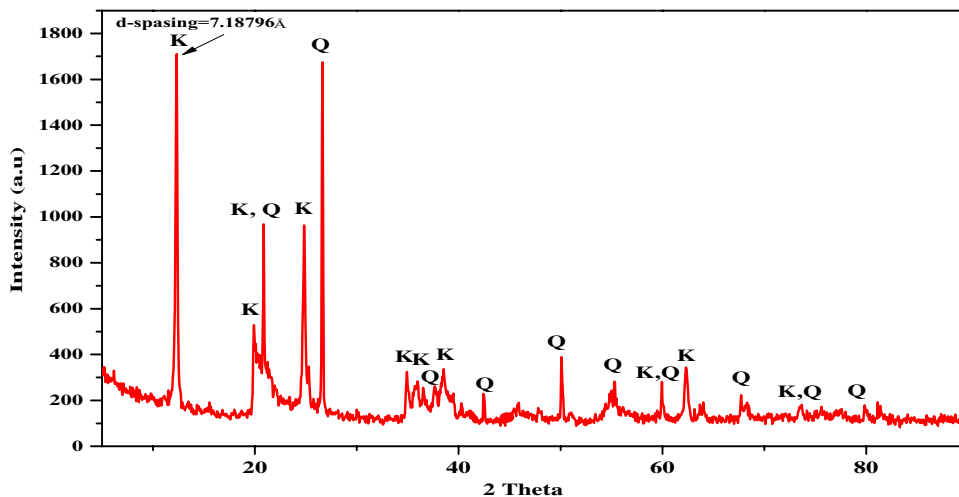
Within the structure of this natural clay, the main peaks appeared in the  $2\theta$  equal to  $12.31^\circ$ ,  $19.90^\circ$ ,  $24.81^\circ$ ,  $34.90^\circ$ ,  $35.83^\circ$ ,  $38.46^\circ$ , and  $62.30^\circ$  which correspond to the presence of Kaolinite with a chemical structure  $\text{Al}_2\text{Si}_2\text{O}_5(\text{OH})_4$  and an interlayer distance of  $7.18796 \text{ \AA}$ . Other peaks have appeared in the  $2\theta$  equal to  $24.82^\circ$ ,  $26.63^\circ$ ,  $36.56^\circ$ ,  $42.48^\circ$ ,  $50.14^\circ$ ,  $55.36^\circ$ ,  $68.08^\circ$ ,  $73.55^\circ$ , and  $79.96^\circ$  corresponding to the existence of Quartz with a  $\text{SiO}_2$  chemical structure. According to the obtained results, this natural clay has a crystalline structure with the presence of two phases in its structure Kaolinite and Quartz.

#### 3.1.4 FTIR Analysis

The identification of the functional groups in the prepared material before and after adsorption was performed, using a FTIR analysis. Where they are presented in Fig. 2.

The contribution of hydroxyl groups found on the edges of the kaolin clay platelets explains the existence of

**Fig. 1** XRD patterns of natural clay (K: Kaolinite; Q: Quartz)



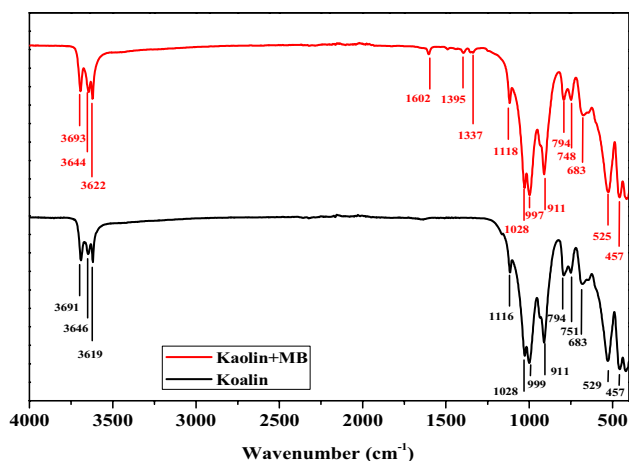


**Fig. 2** FTIR spectra of natural clay before and after adsorption of MB dye

absorption band at  $3691\text{ cm}^{-1}$ . The band at  $3646\text{ cm}^{-1}$  could be connected to the stretching vibration of O–H in water. The band occurring at  $3619\text{ cm}^{-1}$  is due to the stretching vibration of the –OH in the kaolinite sheet attached to aluminum [24, 25]. The bands found at  $1116\text{ cm}^{-1}$  and  $999\text{ cm}^{-1}$  can be explained by the Si–O–Si stretching vibrations of kaolinite or quartz [24]. As for the band occurring at  $1028\text{ cm}^{-1}$  is attributed to the Si–O stretching vibrations [25]. While the Si–O stretching vibration of Quartz [25], clarifies the appearance at  $751\text{ cm}^{-1}$ . After the adsorption of MB dye by the natural clay, a shift was observed in the absorption range bands in the clay structure, which may indicate the interaction between the functional groups in the clay structure and the MB molecules. Furthermore, as a result of the adsorption process of the MB dye, the absorption band appears in the range of  $1602, 1395,$  and  $1337\text{ cm}^{-1}$  in the natural clay structure, which stands for respectively the stretching of –C=C–,

C=N- and –C–N- in Poly heterocycles, showing the adsorption of the MB dye molecules on the clay surface [26, 27].

### 3.1.5 SEM and EDX Analysis

The SEM coupled with EDX were applied to detect the morphological structure and elemental analysis of the natural clay sample, the obtained results are illustrated in Fig. 3, where the SEM image of the natural clay indicates the presence of a smooth surface within the material, characterized by a fine particle, and almost of a regular shape.

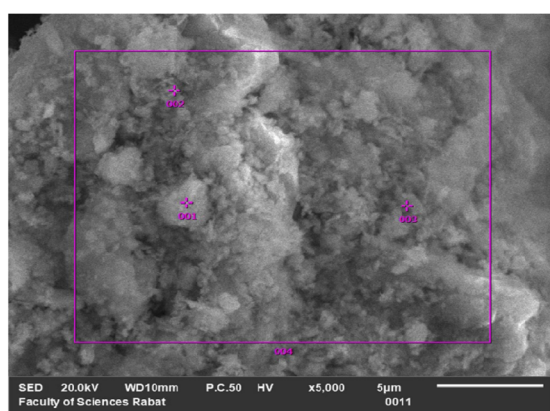
The EDX spectrum of natural clay is presented in Fig. 3, showing that the natural clay contains different elements in various proportions such as O (55.19%), Si (25.67%), Al (13.77%), Fe (2.88%), Ti (1.34%), K (0.74%), Mg (0.21%), and Na (0.21%).

## 3.2 Batch Mode Adsorption of MB

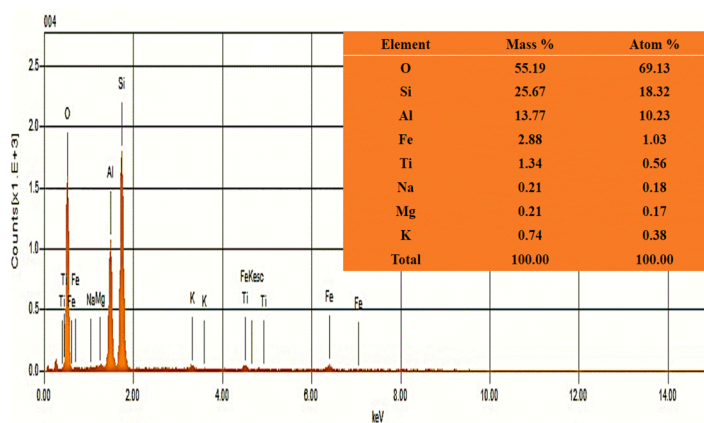
### 3.2.1 Effect of the Adsorbent Dose

In order to determine the effect of adsorbent mass on the adsorption process, an investigation was carried out on the removal of MB dye onto the surface of a natural clay by varying the dosage of clay in an aqueous medium polluted with MB using a  $20\text{ mg L}^{-1}$  concentration, 7.43 solution pH, 120 min of contact time and  $20\text{ }^{\circ}\text{C}$  as a temperature Fig. 4.

Figure 4 reveals that the MB elimination percentage increases rapidly from 28.53 to 99.04% following an increase of natural clay from 0.025 to 0.1 g/50 mL, and then hits a plateau. In fact the percentage of MB dye removed was enhanced with the increase in the adsorbent dosage, this may be due to the existence of a considerable number of active sites present on the clay surface thereby increasing



(a)



(b)

**Fig. 3** SEM micrograph (a) and EDX spectrum (b) of natural clay



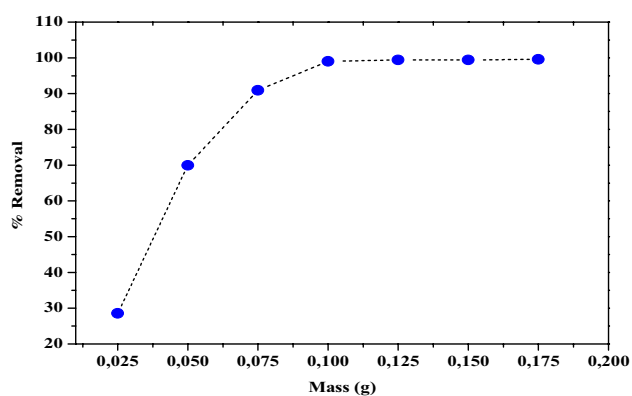


**Fig. 4** Effect of natural clay dosage on removal of MB dye (concentration=20 mg/L, contact time=120 min, temperature=20 °C, adsorbent dosage=0.025–0.175 g/50 mL, pH=7.43)

the contact surface between the MB dye and the surface of the clay [28].

### 3.2.2 Effect of pH

The effect of the pH solution on the removal of MB dye on the clay adsorbent was studied by varying the pH of the aqueous medium from 2.7 to 12 at 20 °C using a fixed dye concentration of 20 mg L<sup>-1</sup>, a fixed contact time of 120 min, and a fixed adsorbent mass of 0.1 g/50 mL, the results are shown in Fig. 5a. The removal of MB dye on kaolin was found to be slightly improved from 97.46 to 99.93% when the pH of the solution increased from 2.7 to 12. The low removal efficiency of MB on clay was obtained at acidic pH rather than basic pH. This is mainly due to the number of

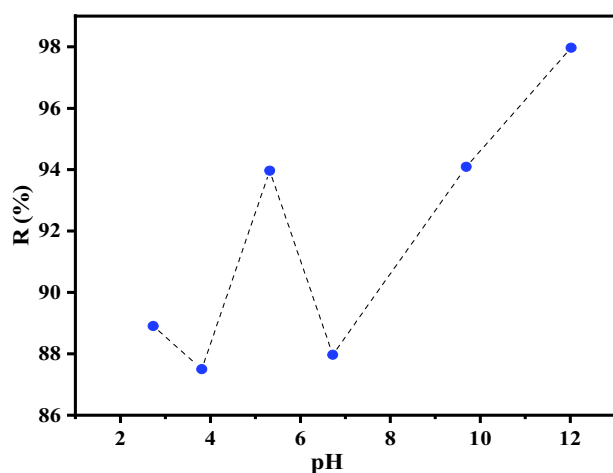
hydrogen ions (H<sup>+</sup>) in the solution, which is high in an acidic solution, filling the active sites, and disfavoring the retention of the cationic dye on the surface of the clay. On the other hand, the strong elimination of the dye seen at high pH is due to the decrease in the number of protons (H<sup>+</sup>) occupying the active sites, and also to the higher negative charge of the adsorbent. Equivalent results have been documented in other studies [29]. The zero-charge point (pHpzc) was established to provide some information on the natural clay adsorbent's surface charge.

The pHpzc of the natural clay is shown in Fig. 5b. It is observed that the zero charge point corresponds to a pH of approximately 7.2. What this shows is at pH below 7.2, there is a net positive charge on the surface of the natural clay, while at pH above 7.2, there is a net negative charge on the surface of the natural clay [30]. Taking into account the nature of the pH of the solution polluted with MB dye, various probable adsorption mechanisms including electrostatic interaction,  $n-\pi$  interaction, ion exchange, hydrogen bonding, and acid–base interaction were suggested to provide an explanation for the interactions between the clay surface, and the dye molecules in the aqueous phase.

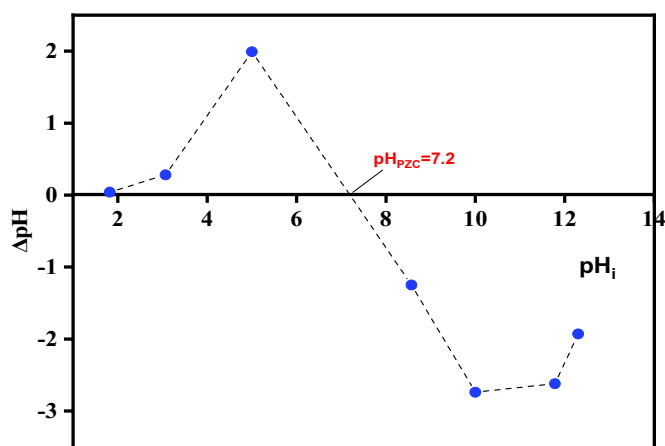
### 3.2.3 Effect of Contact Time and Initial Concentration of Dye

The influences of contact time and initial concentration were tested for the adsorption of MB dye onto kaolin clay.

As shown in Fig. 6 the quantity of the MB dye was adsorbed rapidly in the first 10 min of contact time which was about 9.992 mg g<sup>-1</sup> for 20 mg L<sup>-1</sup>, and reaching about 14.49 mg g<sup>-1</sup>, and 16.19 at 30 min of contact time for



(a)



(b)

**Fig. 5** Effect of pH of solution on removal of MB dye (concentration=20 mg/L, contact time=120 min, temperature=20 °C, adsorbent dosage=0.1 g/50 mL, pH=2.7–12) (a) and pH<sub>pzc</sub> of natural clay (b)

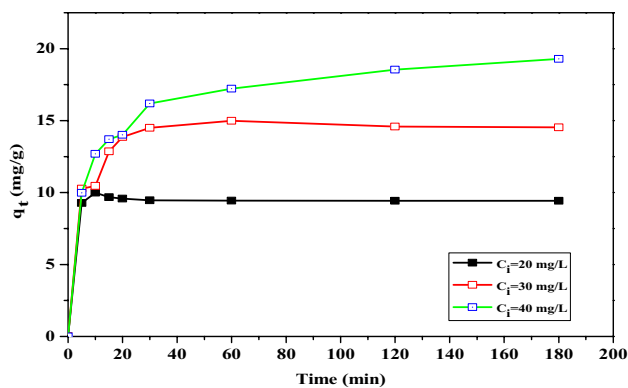


**Fig. 6** Effects of contact time and initial concentration on the adsorption of MB dye (concentration=20, 30 and 40 mg/L, contact time=0 to 180 min, temperature=20 °C, adsorbent dosage=0.1 g/50 mL, pH=7.43)

30 mg L<sup>-1</sup> and 40 mg L<sup>-1</sup>, respectively. then, after that, the adsorbed amount remains nearly constant for the concentration of 20 mg L<sup>-1</sup> and gradually slows down until equilibrium is reached at 14.535 mg g<sup>-1</sup> for 30 mg L<sup>-1</sup> and 19.29 mg g<sup>-1</sup> for 40 mg L<sup>-1</sup>. During the initial phase, the behavior of dye adsorption is rapid, which can be explained by the existence of many active sites on the surface of the clay, over time, these sites become saturated, triggering forces between the MB molecules on the clay surface [31, 32]. Moreover, in Fig. 6 it was noticed that the adsorption of MB dye on the surface of the clay goes from 9.992

to 19.29 mg g<sup>-1</sup> as the initial concentration of MB dye increases from 20 to 40 mg L<sup>-1</sup>. The increased concentration of MB dye in an aqueous medium enhances the interaction between the dye molecules and the kaolin surface and provides the driving force to move the molecules of MB dye from an aqueous solution towards the active sites on the clay surface [33].

### 3.3 Adsorption Kinetic Studies

Adsorption kinetics of MB dye on the clay was achieved during a contact time range of 0–180 min, the results obtained are illustrated in Fig. 7a, b. The kinetic parameters are summarized in Table 1.

The results obtained from the experiment show that, the correlation coefficient (R<sup>2</sup>) of the PSO model was higher than the PFO model and closer to one. The calculated q<sub>e,cal</sub> values was well fitted with the experimental q<sub>e,exp</sub> values for all MB dye concentrations (20, 30, and 40 mg/L). according to this data the PSO model can be considered as the best to describe the adsorption of the MB dye on the surface of the kaolin adsorbent [34] (see Tables 1, 2).

### 3.4 Adsorption Isotherm Studies

Adsorption isotherms of MB dye on natural clay were performed during initial concentrations of the dye in the range of 20 and 80 mg L<sup>-1</sup>. The linear curves of the Langmuir, Freundlich, and Temkin models are given in Fig. 8. The

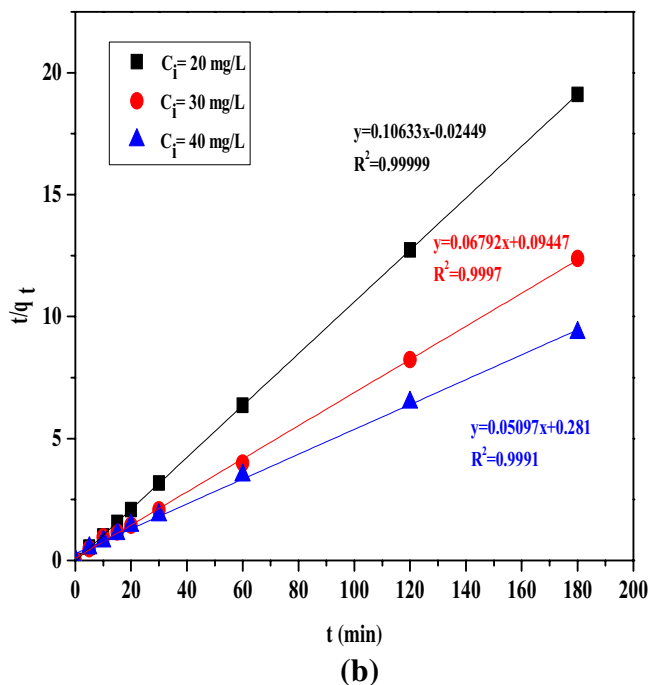
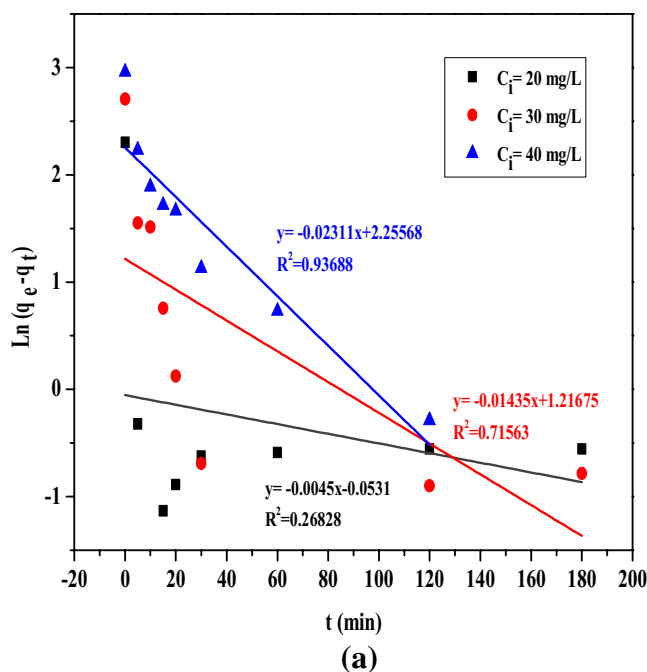


**Fig. 7** Kinetic model for MB dye adsorption using natural clay **a** PFO and **b** PSO

**Table 1** Pseudo-first order and Pseudo-second order parameters for the removal of MB dye onto natural clay

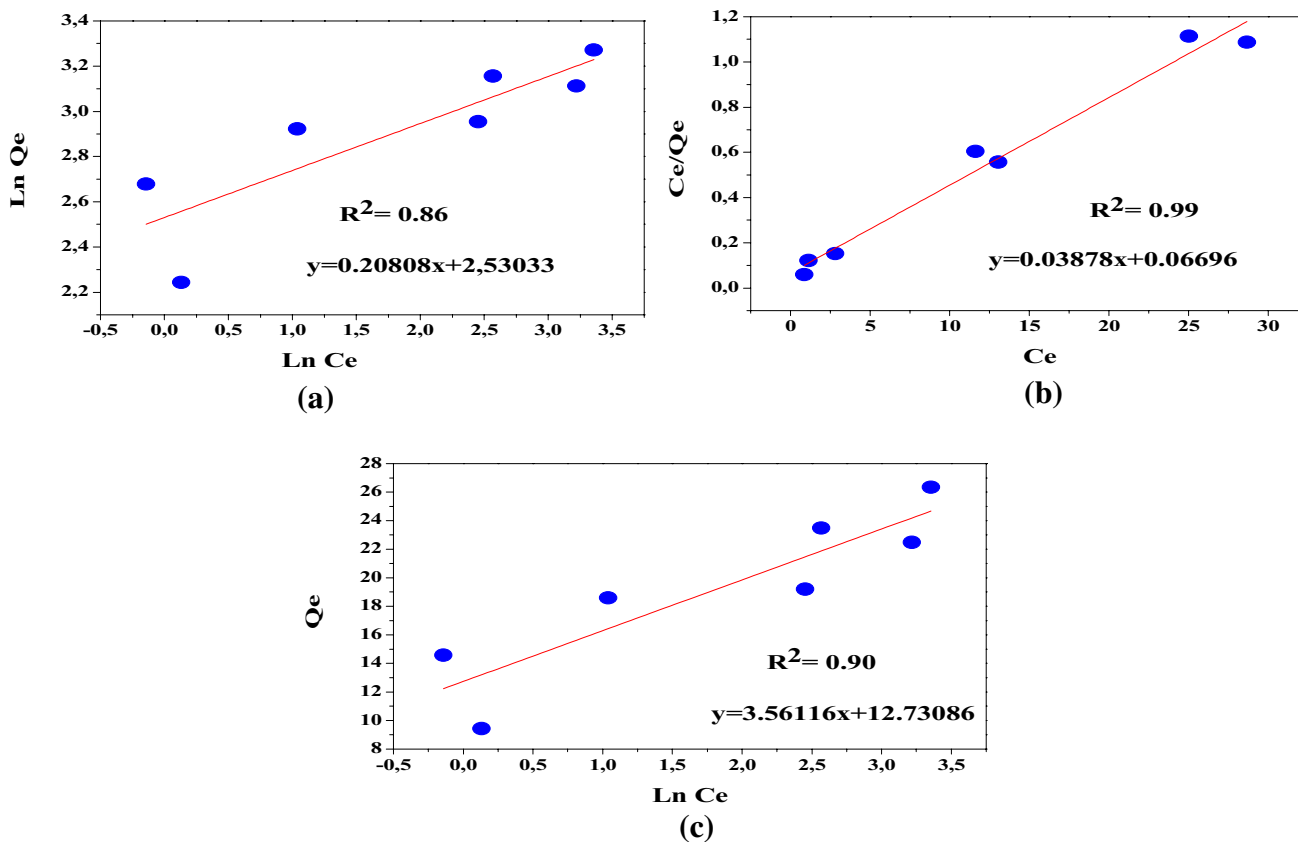
Kinetic models	Parameters	Initial concentration of dye (mg/L)		
		20	30	40
Pseudo-first-order	$R^2$	0.26838	0.711563	0.93688
	$K_1$	0.0045	0.01435	0.02311
	$q_{e,cal}$	0.9482	3.37619	9.54177
	$q_{e,exp}$	9.455	14.992	19.29
Pseudo-second-order	$R^2$	0.99999	0.9997	0.9991
	$K_2$	-0.4616	0.0488	0.0092
	$q_{e,cal}$	9.4046	14.723	19.619
	$q_{e,exp}$	9.455	14.992	19.29

values and constants of these isotherm models are illustrated in Table 3.

As can be seen in Table 3, the  $R^2$  value obtained for the Langmuir isotherm model ( $R^2=0.99$ ) is higher than that of Temkin ( $R^2=0.90$ ) and Freundlich ( $R^2=0.86$ ) isotherm models, which implies a well-fitted adsorption of MB molecules on natural clay according to the Langmuir isotherm model, and thus indicates that the adsorption of MB dye is in a monolayer. It should be noted that most of the isotherm adsorption studies of MB on various adsorbents follow the Langmuir isotherm model [35–38]. Moreover, the maximum amount adsorbed of MB dye on the surface of clay ( $q_{max}$ ) was found to be  $25.79 \text{ mg g}^{-1}$  at  $20 \text{ }^\circ\text{C}$ . The value of  $R_L$

**Table 2** Intraparticle diffusion model parameters for the removal of MB dye onto natural clay

Initial concentration of dye (mg/L)	Intraparticle diffusion model parameters					
	$kin_{,1}$ (mg/g. min <sup>0.5</sup> )	$I_1$ (mg/g)	$kin_{,2}$ (mg/g. min <sup>0.5</sup> )	$I_2$ (mg/g)	$kin_{,3}$ (mg/g. min <sup>0.5</sup> )	$I_3$ (mg/g)
20	3.50124	0.1197	–	–	-0.02114	9.65818
30	3.80325	0.06459	1.01453	9.0622	-0.01372	14.7794
40	3.762	0.371	1.5198	7.6950	0.39369	14.10738

**Fig. 8** Isotherm model for MB dye adsorption using natural clay **a** Langmuir, **b** Freundlich and Temkin (c)



**Table 3** Freundlich, Langmuir, and Temkin parameters for the removal of MB dye onto natural clay

	Parameters	Values
Langmuir	$q_{\max}$ (mg/g)	25.79
	$K_L$ (L/mg)	0.58
	$R^2$	0.99
	$R_L$	0.021–0.079
Freundlich	$K_f$ (mg/g)	12.56
	$n$	4.81
	$R^2$	0.86
Temkin	$B$ (J/mol)	3.56
	$K_T$ (L/mg)	25.52
	$R^2$	0.90

parameter ( $0 < R_L < 1$ ) shows a favorable adsorption process of MB dye.

The adsorption capacity ( $q_{\max}$ ) of the Langmuir model isotherm of MB dye on kaolin clay, compared to a selection of other clay adsorbents in the literature is depicted in Table 4. It can be seen that the Mauritanian natural clay presents a satisfactory performance and a good efficiency for the removal of MB in an aqueous medium than the other clays reported in the literature. It is important to note that the preparation of our natural clay adsorbent required less energy and has not undergone any chemical modification.

### 3.5 Adsorption Mechanisms

The adsorption of MB onto kaolin adsorbent is an overly complex process, a several interactions coexist during the process. Under the influence of pH, in an acidic environment,  $H^+$  ions occupy the negatively charged siloxane group of the clay. Which assume that the interactions between the clay surface charged negatively and the positive charge of dye fall under van der Waals forces, hydrogen bonds, and  $n-\pi$  interactions. The clay surface silanol groups are more deprotonated (Si–O<sup>-</sup>) in the basic medium, indicating that

**Table 4** Comparison of the adsorption capacity of MB dye by various adsorbents

Adsorbents	$Q_{\max}$ (mg g <sup>-1</sup> )	References
Raw kaolin	14	[39]
Natural zeolite	21.78	[40]
Zeolite (raw clay)	8.67	[41]
Natural zeolite	19.9	[42]
Moroccan Illitic clay	13.69	[43]
Raw coal fy ash	5.06	[44]
Red-clay	18.83	[45]
Mauritanian natural kaolin clay	25.79	This work

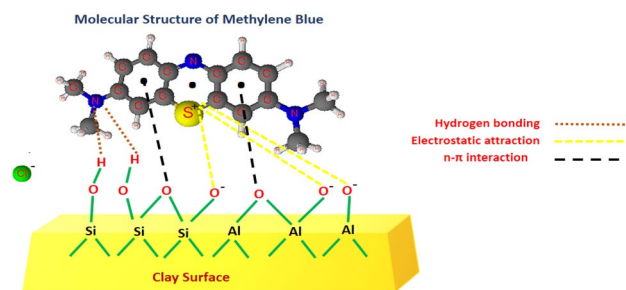
the interaction between the functional groups on the clay surface, which are negatively charged, and the MB molecules, which are positively charged, is electrostatic. [30]. According to the results of the FTIR spectra, the absorption peak intensities of the clay changed after the adsorption of MB, the apparition of new characteristic absorption peaks suggests that these functional groups contributed to the adsorption process, while there are physical–chemical changes taking place. For example, the electrostatic interaction was confirmed by the apparition of a new peak found at 1395 and 1337 cm<sup>-1</sup>. The adsorption of MB molecules on the clay surface under the action of hydrogen bonding was confirmed by the peak shift around 3691 cm<sup>-1</sup> to 3693 cm<sup>-1</sup> (O–H stretching vibration). In addition, it was discovered that O–H, Si–O, Al–OH, and Si–O–Si bend in the structure of kaolin clay handled the removal of MB dye from aqueous solution as can be elucidated in Fig. 2. As a result, from the FTIR characterization analysis and the pH solution effect, the MB cationic dye appears to be adsorbed on the clay surface through electrostatic interaction, Van Der Waals forces and  $n-\pi$  interaction. The proposed mechanism for the adsorption of MB dye on the natural clay is presented in Fig. 9.

### 3.6 Adsorption Thermodynamics Studies

The thermodynamic parameters such as ( $\Delta G^\circ$ ), ( $\Delta H^\circ$ ) and ( $\Delta S^\circ$ ) were calculated by the equation presented in Fig. 10.

The values of these parameters are written in Table 5. Based on the  $\Delta G^\circ$  values at different level of temperatures, it is clair indicated, the feasibility and spontaneity of the retention of MB dye onto kaolin adsorbent.

Therefore, the  $\Delta G^\circ$  values (between -4.24 kJ.mol<sup>-1</sup> and -3.85 kJ.mol<sup>-1</sup>) exist in the range of -20 and 0 kJ.mol<sup>-1</sup>, which assume the physisorption nature for the uptake of MB onto kaolin clay [46]. Moreover, the negative  $\Delta H^\circ$  (-1.41 kJ mol<sup>-1</sup>) value reveals the exothermic adsorption process, and The positive value of  $\Delta S^\circ$  (13.13 J mol<sup>-1</sup> K<sup>-1</sup>) shows a random increase in the aqueous medium during the reaction between MB molecules and the natural clay surface. [46]. to conclude, the thermodynamic study confirme the

**Fig. 9** Proposed mechanism for adsorption of MB dye on the natural clay

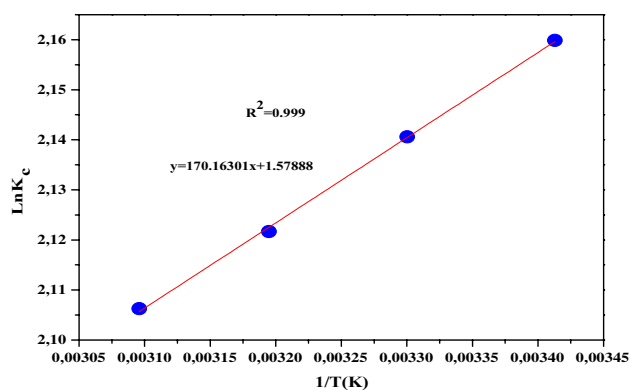


**Fig. 10** Enthalpy and entropy change the determination of the adsorption of MB dye onto natural clay

**Table 5** Thermodynamic parameters for removal of MB dye onto natural clay

Thermodynamic parameters				
$\Delta H^\circ$ (kJ mol <sup>-1</sup> )	- 1.41			
$\Delta S^\circ$ (J mol <sup>-1</sup> K <sup>-1</sup> )	13.13			
$\Delta G^\circ$ (kJ mol <sup>-1</sup> )	20 °C	30 °C	40 °C	50 °C
	- 3.85	- 3.98	- 4.11	- 4.24

spontaneity, feasibility and exothermic physisorption nature of the MB dye adsorption onto kaolin clay.

### 3.7 The Reusability of the Adsorbent

Regeneration is very important aspect of the adsorption from economy and environmental point of view. The regeneration can reduce the need of new adsorbent and also reduce the problem of disposal of used adsorbent. Various regeneration methods have been used with different degrees of success. These methods includes solvent washing, thermal, chemical and electrochemical regeneration. However, according to Aguedal et al. [47], the thermal treatment is an effective method of treatment which lead to enhance the adsorption capacities of diatomite and promote the possibilities for material recovery and recycling.

The desorption and regeneration of kaolin clay was depicted in Fig. 11. The efficiency removal decreases from 96.74 to 71.92% after a continuous regeneration after 4th cycle of reuse (5th adsorption test). The efficiency of MB removal by the adsorption process on thermally recycled clay decreased slightly, which may be due to the lack of active sites on the surface of the adsorbent, thereby decreasing the chemical and physical solute/solid interactions. As a result, this natural kaolin clay can be considered a promising, efficient and regenerable adsorbent for the removal of MB as cation dyes from an aqueous medium. Furthermore,

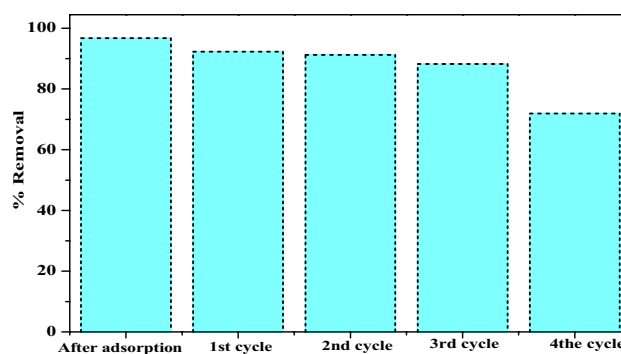


**Fig. 11** Adsorption process of MB dye after several cycles of adsorption/desorption using natural clay

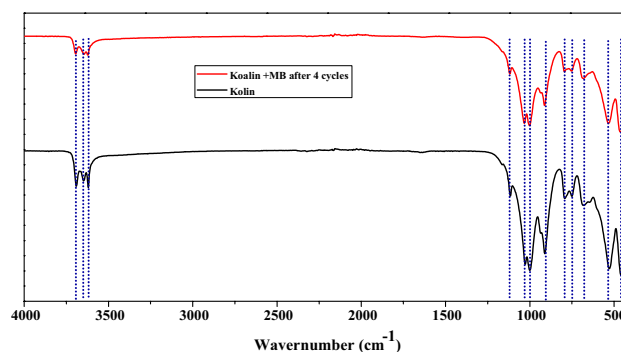


**Fig. 12** FTIR analysis of natural clay and the reusability after 4 cycles

to assess the change in functional groups on the clay surface before and after recycling adsorption process, a FTIR analysis was conducted.

Figure 12 depicts the FTIR spectra of the clay adsorbent before and after the 4 cycles of regeneration.

According to the FTIR spectrum Fig. 12, it can be seen that the clay sample even after the 4th cycle, the position of all bands remains the same without any changes in their positions, further It was also found that the intensity of the bands changed slightly after using the recycled material. This change in intensity can be explained by the thermal degradation of MB molecules that are physically attached to the clay surface. DSC analysis was conducted to identify the temperature at which the dihydroxylation of the kaolin occurred as well as the metakaolin formation, followed by an evaluation of the stability of the clay after the recycling process.

Figure 13 presents the results of the thermal analysis of kaolin before and after 4th thermal recycling process. The endothermic peak in the temperature between 400 and 650 °C corresponds to the dihydroxylation of the kaolinite, and the temperature of decomposition is located at 516 °C [48]. The fixation of MB on kaolin surface can be

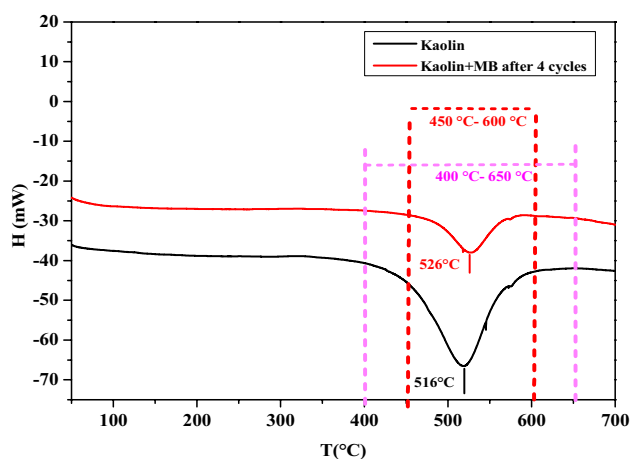


**Fig. 13** DSC curve of natural clay and the reusability after 4 cycles

explained by a decrease around the hydroxylation peak of kaolin located between 400 and 650 °C to the area between 450 and 600 °C, and the increase in the H<sub>2</sub>O decomposition temperature of kaolin at 526–516 °C after the 4th thermal recycling which occurred without structural deformation. the FTIR study confirmed the preservation of kaolin structure after the 4 th thermal recycling at 400 °C.

## 4 Conclusions

This research focused on the use of Mauritanian kaolin clay, as a natural available source to remove methylene blue from the aqueous environment. An investigation of several parameters influencing MB's adsorption on clay were performed. Additionally, the Langmuir model has the potential to be well-fitted the adsorption of MB dye onto kaolin on which the adsorption capacity was 25.79 mg g<sup>-1</sup> at 20 °C. The pseudo-second-order model best represented the adsorption kinetics. The thermodynamic data collected indicate the exothermic and spontaneous physisorption nature of the process. Furthermore, the results show that the thermal regeneration of the clay could be up to four consecutive cycles of successful regeneration without change in its structure.

## Declarations

**Conflict of Interest** The authors declare that there is no conflict of interest.

## References

1. Archana S, Radhika D, Jayanna B, Kannan K, Kumar KY, Muralidhara H (2021) Functionalization and partial grafting of the reduced graphene oxide with p-phenylenediamine: an adsorption and photodegradation studies. *FlatChem* 26:100210

2. Saufi H, El Alouani M, Alehyen S, El Achouri M, Aride J (2020) Photocatalytic degradation of methylene blue from aqueous medium onto perlite-based geopolymer. *Int J Chem Eng* 1–7
3. Gadekar MR, Ahammed MM (2016) Coagulation/flocculation process for dye removal using water treatment residuals: modelling through artificial neural networks. *Desalin Water Treat* 57:26392–26400
4. Al-Bastaki N (2004) Removal of methyl orange dye and Na<sub>2</sub>SO<sub>4</sub> salt from synthetic waste water using reverse osmosis. *Chem Eng Process* 43:1561–1567
5. Nidheesh P, Zhou M, Oturan MA (2018) An overview on the removal of synthetic dyes from water by electrochemical advanced oxidation processes. *Chemosphere* 197:210–227
6. Venkatesh S, Venkatesh K, Quaff AR (2017) Dye decomposition by combined ozonation and anaerobic treatment: cost effective technology. *J Appl Res Technol* 15:340–345
7. El-Ashtouky E-S, Fouad Y (2015) Liquid–liquid extraction of methylene blue dye from aqueous solutions using sodium dodecylbenzenesulfonate as an extractant. *Alex Eng J* 54:77–81
8. Zhang Y, Yu W, Li R, Xu Y, Shen L, Lin H, Liao B-Q, Wu G (2019) Novel conductive membranes breaking through the selectivity-permeability trade-off for Congo red removal. *Sep Purif Technol* 211:368–376
9. Bal D, Özer Ç, İmamoğlu M (2021) Green and ecofriendly bio-char preparation from pumpkin peel and its usage as an adsorbent for methylene blue removal from aqueous solutions. *Water Air Soil Pollut* 232:1–16
10. Hamad HN, Idrus S (2022) Recent developments in the application of bio-waste-derived adsorbents for the removal of methylene blue from wastewater: a review. *Polymers* 14:783
11. El hadj Ali Y, Demba N'diaye A, Ahrouch M, Sakar EH, Raklami A, Lahcen AA, Stitou M (2022) Dehydrate sewage sludge as an efficient adsorbent for malachite green removal in textile wastewater: experimental and theoretical studies. *Chem Afr* 5:359–373
12. Srivastava A, Gupta B, Majumder A, Gupta AK, Nimbhorkar SK (2021) A comprehensive review on the synthesis, performance, modifications, and regeneration of activated carbon for the adsorptive removal of various water pollutants. *J Environ Chem Eng* 9:106177
13. Leiviskä T, Sarpola A, Tanskanen J (2012) Removal of lipophilic extractives from debarking wastewater by adsorption on kaolin or enhanced coagulation with chitosan and kaolin. *Appl Clay Sci* 61:28
14. Leiviskä T, Sarpola A, Heikkinen E, Tanskanen J (2013) Thermal properties and phosphate adsorption efficiency of coarse aluminum silicate fraction. *Desalin Water Treat* 51(34–36):6837–6845
15. Hamza W, Dammak N, Hadjtaief HB, Eloussaief M, Benzina M (2018) Sono-assisted adsorption of crystal violet dye onto tunisian smectite clay: characterization, kinetics and adsorption isotherms. *Ecotox Environ Safe* 163:365–371
16. Tariq R, Abatal M, Bassam A (2022) Computational intelligence for empirical modeling and optimization of methylene blue adsorption phenomena using available local zeolites and clay of Morocco. *J Clean Prod* 370(10):133517
17. Aoulad El Hadj Ali Y, Ahrouch M, Ait Lahcen A, Demba N'diaye A, El Yousfi F, Stitou M (2021) Dried sewage sludge as an efficient adsorbent for pollutants: cationic methylene blue removal case study. *Nanotechnol Environ Eng* 6:1–13
18. N'diaye AD, Ali YAEH, Bollahi MA, Stitou M, Kankou M, Fahmi D (2020) Adsorption of Methylene Blue from aqueous solution using Senegal River *Typha australis*. *Mediterr J Chem* 10:22–32
19. Balarak D, Jaafari J, Hassani G, Mahdavi Y, Tyagi I, Agarwal S, Gupta VK (2015) The use of low-cost adsorbent (*Canola residues*) for the adsorption of methylene blue from aqueous solution:

- Isotherm, kinetic and thermodynamic studies. *Colloids Interface Sci Commun* 7:16–19
20. Qlihaa A, Dhimni S, Melrhaka F, Hajjaji N, Srhiri A (2016) Caractérisation physico-chimique d'une argile Marocaine. *J Mater Environ Sci* 7(5):1741–2175
  21. Moyo M, Chikazaza L, Nyamunda BC, Guyo U (2013) Adsorption batch studies on the removal of Pb (II) using maize tassel based activated carbon. *J Chem* 508934:8
  22. El Alouani M, Alehyen S, El Achouri M, Taibi M (2019) Preparation, characterization, and application of metakaolin-based Geopolymer for removal of Methylene Blue from aqueous solution. *J Chem* 2019
  23. El Alouani M, Saufi H, Moutaoukil G, Alehyen S, Nematollahi B, Belmaghraoui W, Taibi MH (2021) Application of geopolymers for treatment of water contaminated with organic and inorganic pollutants: state-of-the-art review. *J Environ Chem Eng* 9:105095
  24. Mouni L, Belkhiri L, Bollinger JC, Bouzaza A, Assadi A, Tirri A, Dahmoune F, Madani K, Remini H (2018) Removal of Methylene Blue from aqueous solutions by adsorption on Kaolin: Kinetic and equilibrium studies. *Appl Clay Sci* 153:38–45
  25. Sarma G, Sen GS, Bhattacharyya K (2019) Removal of hazardous basic dyes from aqueous solution by adsorption onto kaolinite and acid-treated kaolinite: kinetics, isotherm and mechanistic study. *SN Appl Sci* 1:1–15
  26. Sakin Omer O, Hussein MA, Hussein BHM, Mgaidi A (2018) Adsorption thermodynamics of cationic dyes (methylene blue and crystal violet) to a natural clay mineral from aqueous solution between 293.15 and 323.15 K. *Arab J Chem* 11:615–623
  27. Khan MI (2020) Adsorption of methylene blue onto natural Saudi Red Clay: isotherms, kinetics and thermodynamic studies. *Mater Res Express* 7:055507
  28. Haounati R, Ouachtak H, El Haouti R, Akhouairi S, Largo F, Akbal F, Benlhachemi A, Jada A, Addi AA (2021) Elaboration and properties of a new SDS/CTAB@ Montmorillonite organo-clay composite as a superb adsorbent for the removal of malachite green from aqueous solutions. *Sep Purif Technol* 255:117335
  29. Zhang Y, Wang W, Zhang J, Liu P, Wang A (2015) A comparative study about adsorption of natural palygorskite for methylene blue. *Chem Eng J* 262:390–398
  30. Nwosu FO, Ajala OJ, Owoyemi RM, Raheem BG (2018) Preparation and characterization of adsorbents derived from bentonite and kaolin clays. *Appl Water Sci* 8:1–10
  31. Marrakchi F, Khanday W, Asif M, Hameed B (2016) Cross-linked chitosan/sepiolite composite for the adsorption of methylene blue and reactive orange 16. *Int J Biol Macromol* 93:1231–1239
  32. Aysan H, Edebali S, Ozdemir C, Karakaya MC, Karakaya N (2016) Use of chabazite, a naturally abundant zeolite, for the investigation of the adsorption kinetics and mechanism of methylene blue dye. *Microporous Mesoporous Mater* 235:78–86
  33. Njoku V, Islam MA, Asif M, Hameed B (2014) Preparation of mesoporous activated carbon from coconut frond for the adsorption of carbofuran insecticide. *J Anal Appl Pyrol* 110:172–180
  34. Adeyemo AA, Adeoye IO, Bello OS (2017) Adsorption of dyes using different types of clay: a review. *Appl Water Sci* 7:543–568
  35. Jawad AH, Rashid RA, Mahmuod RMA, Ishak MAM, Kasima NN, Ismail K (2016) Adsorption of methylene blue onto coconut (*Cocos nucifera*) leaf: optimization, isotherm and kinetic studies. *Desalin Water Treat* 19:8839–8853
  36. Jawad AH, Kadhum AM, Ngoh YS (2018) Application of dragon fruit (*Hylocereus polyrhizus*) peels as low-cost biosorbent for adsorption of methylene blue from aqueous solution: kinetics, equilibrium and thermodynamics studies. *Desalin Water Treat* 109:231–240
  37. Jawad AH, Waheeb AS, Rashid RA, Nawawi WI, Yousif E (2018) Equilibrium isotherms, kinetics, and thermodynamics studies of methylene blue adsorption on pomegranate (*Punica granatum*) peels as a natural low-cost biosorbent. *Desalin Water Treat* 105:322–331
  38. Jawad AH, Ngoh YD, Radzun KA (2018) Utilization of watermelon (*Citrullus lanatus*) rinds as a natural low-cost biosorbent for adsorption of methylene blue: kinetic, equilibrium and thermodynamic studies. *J Taibah Univ Sci* 4:371–381
  39. Hang PT, Brindley GW (1970) Methylene blue adsorption by clay minerals. Determination of surface areas and cation exchange capacities (clay-organic studies XVIII). *Clays Clay Miner* 18(4):203–212
  40. Wang S, Zhu Z (2006) Characterisation and environmental application of an Australian natural zeolite for basic dye removal from aqueous solution. *J Hazard Mater* 136:946–952
  41. Jin X, Jiang MQ, Shan X-Q, Pei Z-G, Chen Z (2008) Adsorption of methylene blue and orange II onto unmodified and surfactant-modified zeolite. *J Colloid Interface Sci* 328:243–247
  42. Han R, Zhang J, Han P, Wang Y, Zhao Z, Tang M (2009) Study of equilibrium, kinetic and thermodynamic parameters about methylene blue adsorption onto natural zeolite. *Chem Eng J* 145(3):496–504
  43. Amrhar O, Nassali H, Elyoubi M (2015) Adsorption of cationic dye, methylene blue, onto Moroccan illitic clay. *J Mater Environ Sci* 6:3054–3065
  44. Li H, Dai M, Dai S, Dong X, Li F (2018) Methylene blue adsorption properties of mechanochemistry modified coal fly ash. *Hum Ecol Risk Assess* 24(8):2133–2141
  45. Bentahar Y, Draoui K, Hurel C, Ajouyed O, Khairoun S, Marmier N (2019) Physico-chemical characterization and valorization of swelling and non-swelling Moroccan clays in basic dye removal from aqueous solutions. *J Afr Earth Sci* 154:80–88
  46. Elmoubarki R, Mahjoubi F, Tounsadi H, Moustadraf J, Abdenouri M, Zouhri A, El Albani A, Barka N (2015) Adsorption of textile dyes on raw and decanted Moroccan clays: kinetics, equilibrium and thermodynamics. *Water Resour Ind* 9:16–29
  47. Aguedal H, Iddou A, Aziz A, Shishkin A, Ločs J, Juhna T (2018) Effect of thermal regeneration of diatomite adsorbent on its efficacy for removal of dye from water. *Int J Environ Sci Technol*. <https://doi.org/10.1007/s13762-018-1647-5>
  48. Ondro T, Trník A (2018) Kinetic behaviour of thermal transformations of kaolinite, AIP conference proceedings. AIP Publishing LLC, p 020033

Springer Nature or its licensor (e.g. a society or other partner) holds exclusive rights to this article under a publishing agreement with the author(s) or other rightsholder(s); author self-archiving of the accepted manuscript version of this article is solely governed by the terms of such publishing agreement and applicable law.